S1 Supplementary methods

S1.1 Model specifications

B1 – Avalanche-day climatic conditions. Layer A included each avalanche day once, whereas B1 linked the PC1 scores derived from the pooled Layer A PCA to each path type active on that date, without performing a separate PCA. After excluding the winters 1999/00–2001/02, the analysis included 436 cluster-days from 333 unique avalanche dates. The Period × Cluster interaction was evaluated using a 12-df Wald test, and differences among path types in the P4 − P1 contrasts were assessed using a joint Wald test.

B2 – Recorded path activity. The binomial mixed-effects model included 2,310 path-winters (55 paths × 42 winters) and was fitted by maximum likelihood using the Laplace approximation, with results cross-checked in glmmTMB. The Period × Cluster interaction was evaluated using a 12-df Wald test, and differences among path types in the P4/P1 odds ratios using a 4-df Wald test.

B3 – Avalanche magnitude and geometry. Avalanche area (the primary measure of event magnitude), width, length, crown height and deposit height were log-transformed and analysed using linear mixed-effects models. The analyses included 790 events for area, 791 for width, 792 for length, 782 for crown height and 791 for deposit height. Full and additive models were compared using likelihood-ratio tests based on maximum-likelihood fits. P4/P1 ratios and differences among path types were estimated from models fitted by restricted maximum likelihood.

Large avalanches. The number of large natural avalanche events per winter was compared among periods using negative-binomial generalised linear models, with the overall Period effect evaluated by a likelihood-ratio test. Their share among all recorded natural avalanches was analysed using binomial mixed-effects models with Path and Season random intercepts. Absolute area thresholds were based on the 800 avalanches with recorded area, whereas path-relative thresholds were evaluated for the 790 events with recorded area assigned to mapped avalanche paths.

S1.2 Cluster validation and alternative morphometric typologies

The Caliński–Harabasz index (pseudo-F), pseudo-t^2 and cubic clustering criterion were calculated from within-cluster sums of squares of the standardised rotated component scores. Silhouette width was calculated using the distance measure applied in clustering, and the gap statistic was estimated from 500 reference datasets (Table S2a).

Because Manhattan distances, unlike Euclidean distances, depend on the rotation of the component space, the final morphometric typology was compared with classifications based on Kaiser-normalised Varimax scores and conventional Ward clustering using Euclidean distances (Table S2b).

All Layer B models were also fitted using the four-cluster solution obtained by merging C2 and C3 in the final classification tree (Table S2c).

S1.3 Sensitivity analyses

Layer A was repeated after excluding wind and humidity variables affected by sensor replacement or changes in sensor height at Labská bouda (2002 and 2010). A second analysis included the 47 avalanche days from the winters 1999/00–2001/02 that were excluded from the main analysis because of incomplete meteorological records (Table S3a).

In B1, cluster-days associated with the same avalanche date share identical climatic PC1 scores. To assess the influence of these repeated values, the model was refitted using weights equal to the inverse of the number of path types active on each date and, separately, using only dates with a single active path type. Confidence intervals were also estimated using a whole-winter block bootstrap. A Date random intercept could not be estimated because PC1 was constant within each date (Table S3b).

In B3, the numerical precision of recorded avalanche dimensions changed around 2009/10, as indicated by less frequent rounding in later records. Models were therefore refitted after harmonising width and length to the earlier recording precision (10 m and 50 m, respectively), with avalanche area adjusted accordingly. Additional analyses used only events with non-rounded widths, included a locality random intercept, or were restricted to Obří důl (Table S4).

Recorded path activity (B2) was also reanalysed after excluding the eight paths without recorded natural avalanches in P1 and, separately, after excluding Murová dráha (path 6C; Table S5). B1 and B3 could not be estimated after excluding all eight paths because some Period × Cluster combinations contained no observations.

S2 Supplementary figures

Figure S1. Distribution of the nine climatic variables on recorded natural avalanche days by period (Layer A; 335 avalanche days, excluding the winters 1999/00–2001/02). Boxes show the median and interquartile range, white diamonds indicate the mean, and n denotes the number of avalanche days.

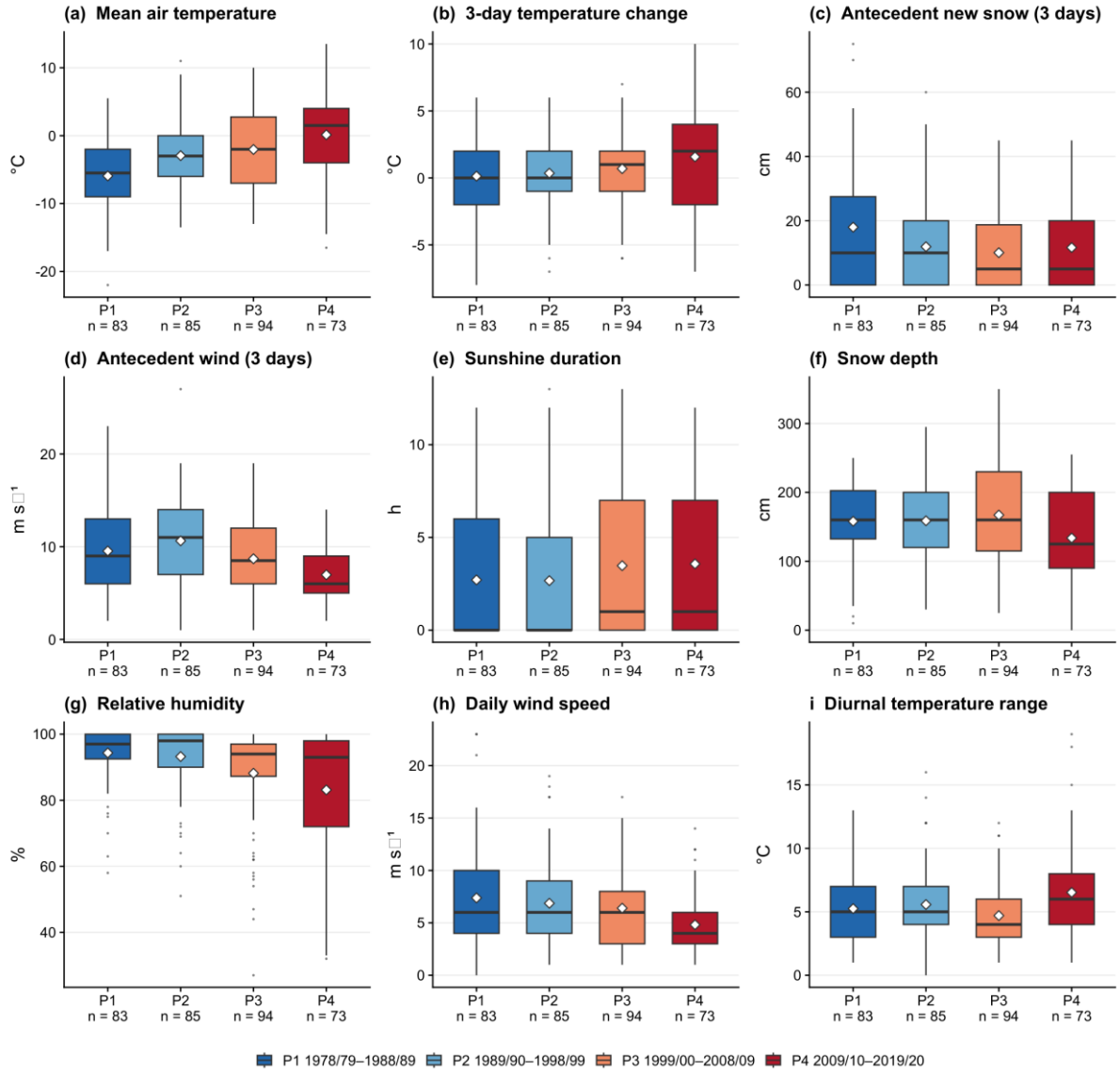


Figure S2. Correlation structure of avalanche-day climatic variables in the earliest (P1, left) and latest (P4, centre) periods, with the change in correlation coefficients between the two periods (P4 − P1, right). Cells show pairwise Pearson correlation coefficients among the nine climatic variables.

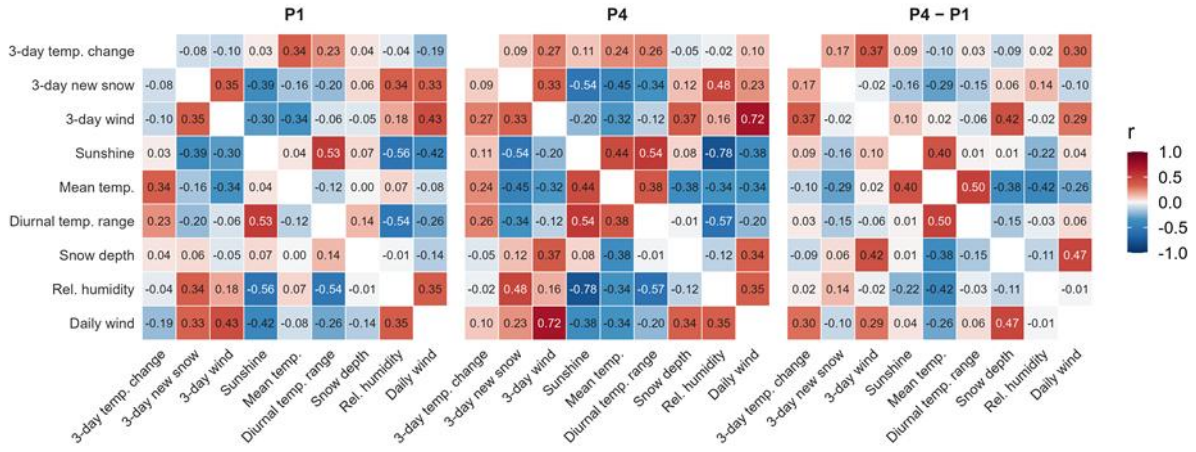


Figure S3. Rotated component loadings of the morphometric PCA based on 13 terrain variables. Five components were retained using the Kaiser criterion and subjected to Varimax rotation without Kaiser normalisation. Loadings with absolute values ≥ 0.5 are shown in bold.

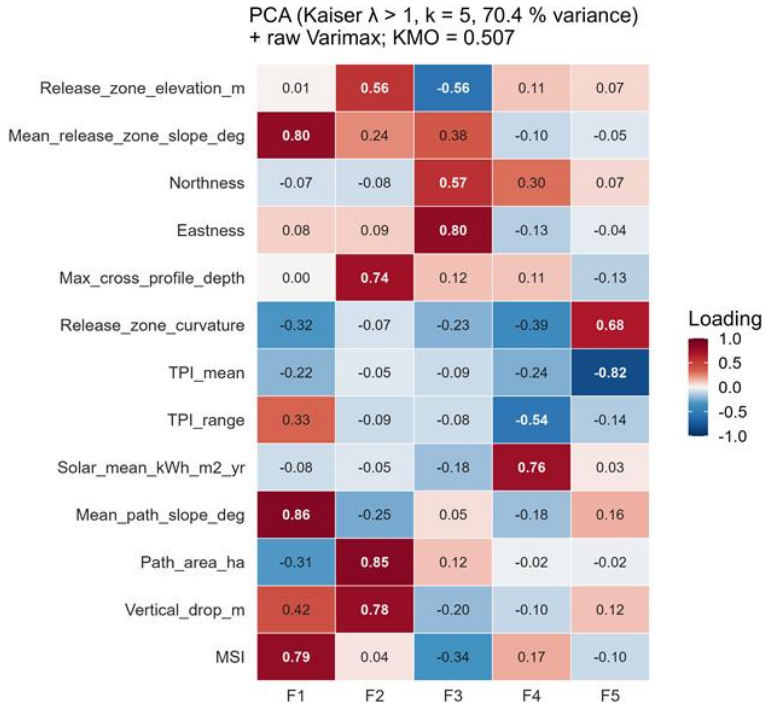


Figure S4. Distribution of avalanche magnitude and geometry by period: (a) avalanche area (logarithmic scale), (b) avalanche length and (c) avalanche width. Boxes show the median and interquartile range, white diamonds indicate the mean, and n denotes the number of recorded natural avalanche events. All periods include the winters 1999/00–2001/02.

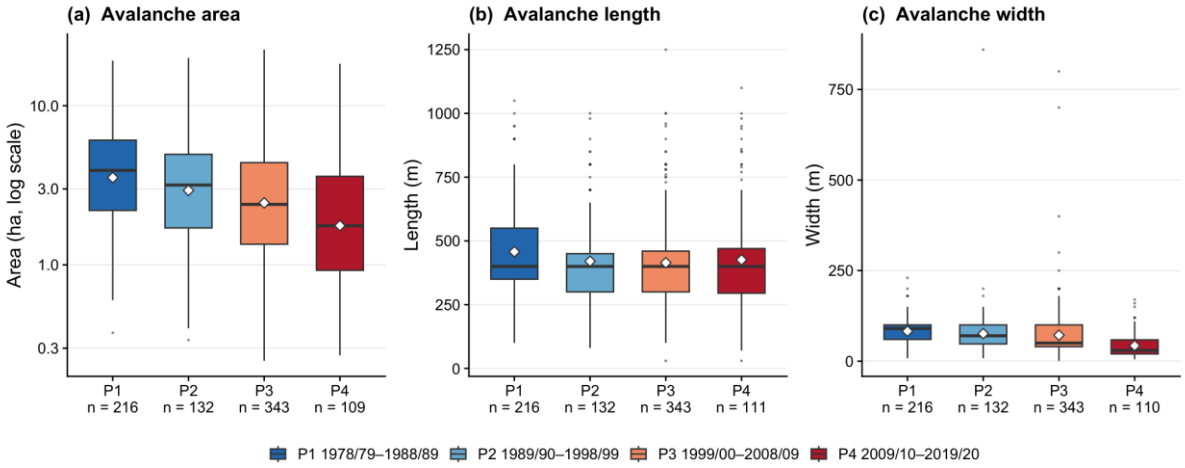


Figure S5. Observed change in the proportion of active winters between P1 and P4 for individual avalanche paths (percentage points). Blue indicates a decrease and red an increase. Paths with fewer than three recorded natural avalanches in P1 and P4 combined are shown in grey. Background: shaded relief.

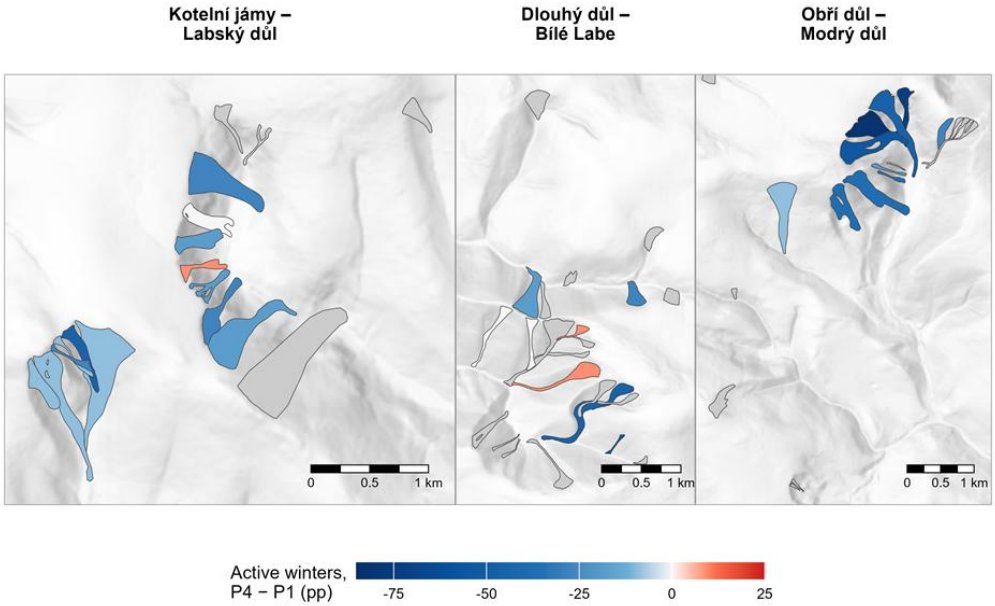


Figure S6. Frequency of large natural avalanche events during 1978/79–2019/20. (a) Number of large avalanches per winter and (b) their share among recorded natural avalanches in P1–P4, using four definitions: area exceeding the 75th (5.0 ha) or 90th (8.1 ha) percentile, and area reaching at least 0.5 or 1.0 times the mapped avalanche-path area. (c) Annual numbers of avalanches exceeding the 90th percentile and of path-overrunning events, with LOESS smoothers. Shading indicates the four study periods.

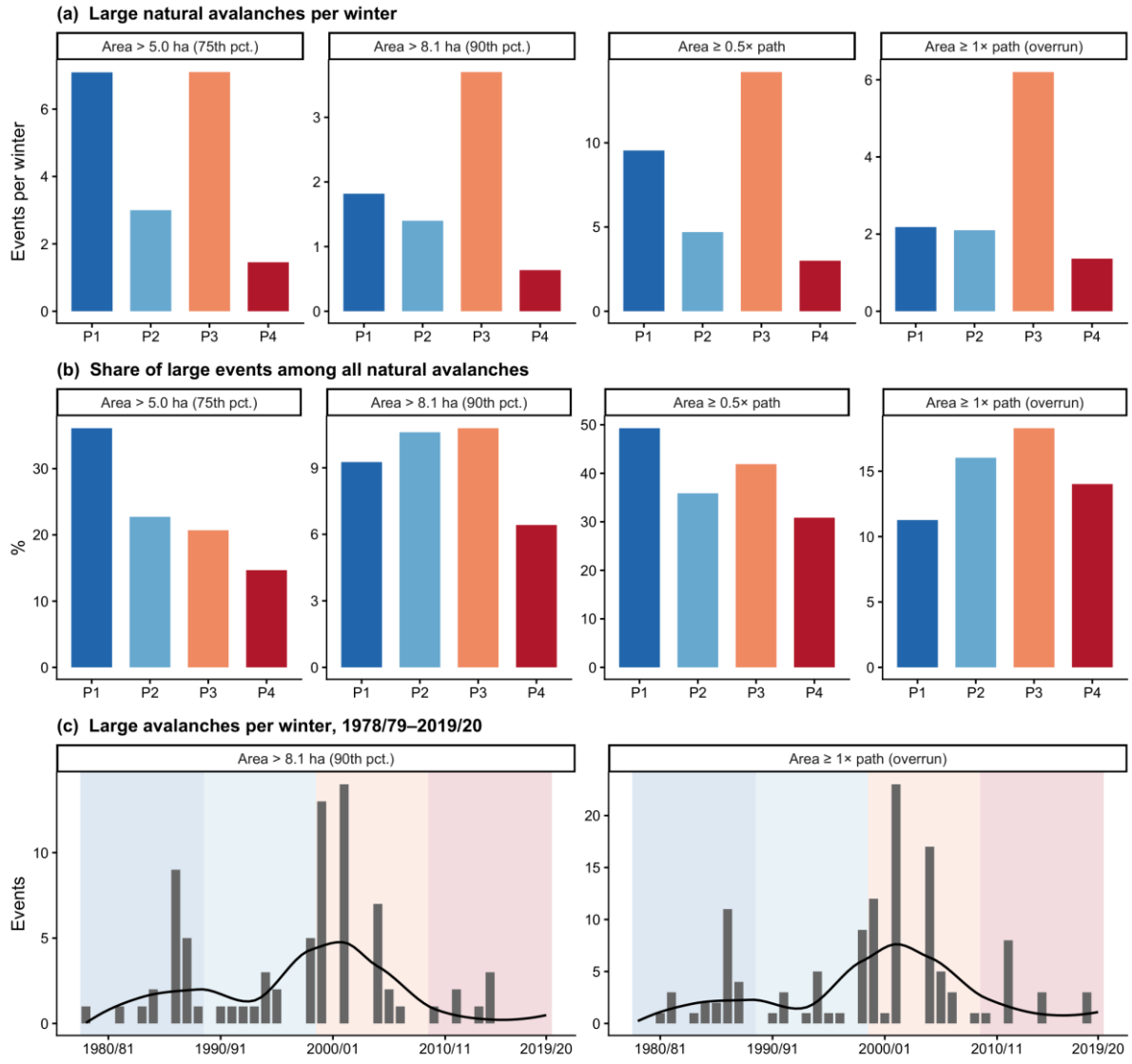
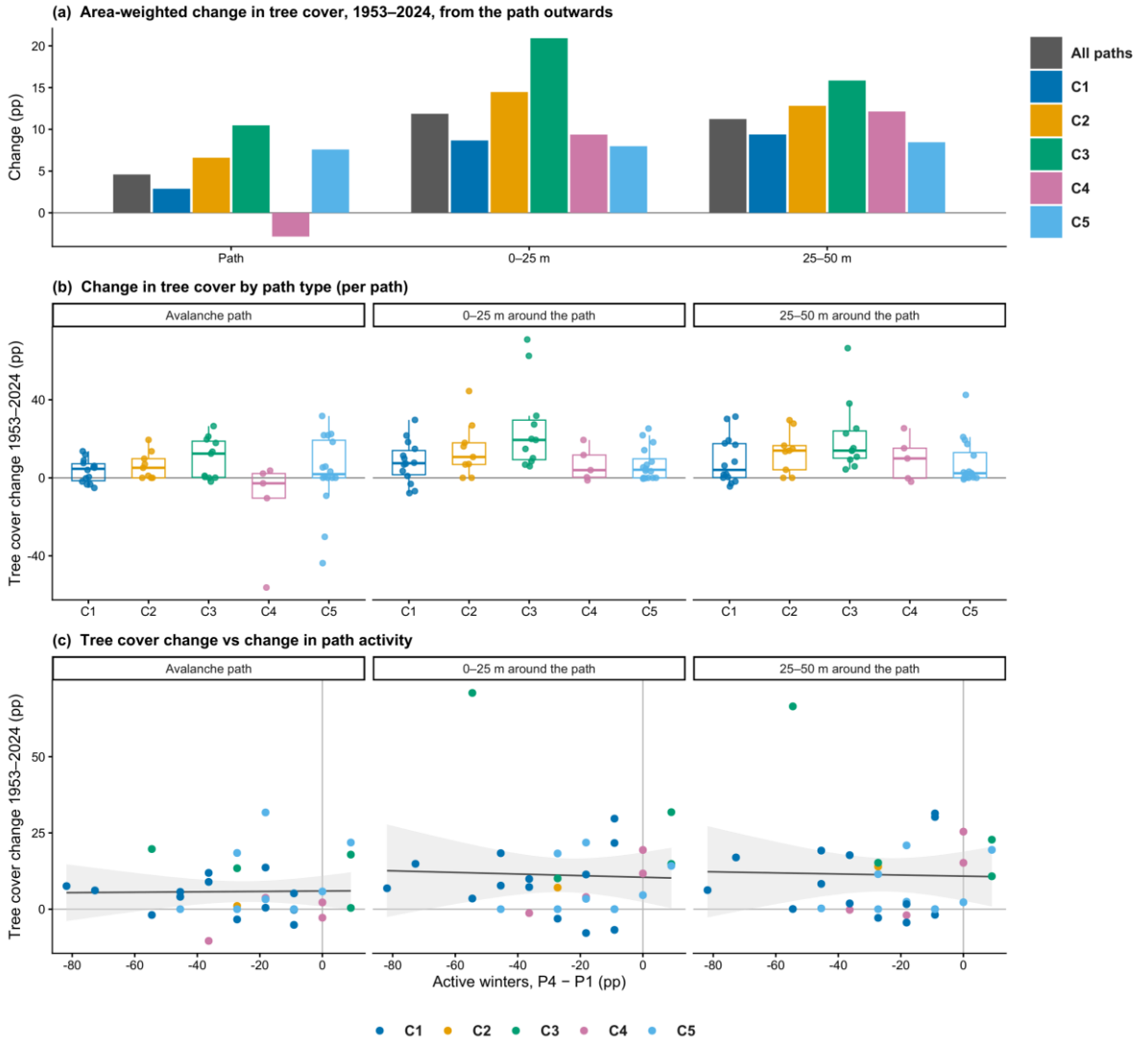


Figure S7. Tree-cover change between 1953 and 2024 within avalanche paths and their surroundings. (a) Area-weighted changes in tree cover within the paths and in the 0–25 m and 25–50 m surrounding zones, for all paths and by morphometric path type. (b) Tree-cover change for individual paths by type. (c) Association between tree-cover change and changes in the proportion of active winters between P1 and P4, restricted to paths with at least three recorded natural avalanches in P1 and P4 combined.



S3 Supplementary tables

Table S1. Morphometric variables used to classify 55 avalanche paths: definitions, derivation methods, units, spatial units and descriptive statistics.

Variable	Definition	Derivation	Unit	Spatial unit	Mean	SD	Min	Max
Release-zone elevation	Mean elevation of the release zone	Zonal mean of the DEM within the release-zone polygon	m a.s.l.	Release zone	1340	78.1	1130	1525
Mean release-zone slope	Mean slope gradient of the release zone	Zonal mean of DEM-derived slope within the release zone	°	Release zone	36.5	6.50	14.5	49.8
Northness	cos(aspect) of the release zone; +1 north, −1 south	cos of the mean release-zone aspect (DEM-derived)	–	Release zone	−0.24	0.70	−1.00	1.00
Eastness	sin(aspect) of the release zone; +1 east, −1 west	sin of the mean release-zone aspect (DEM-derived)	–	Release zone	0.31	0.61	−1.00	1.00
Maximum cross-profile depth	Maximum depth of the release-zone cross profile below its chord; positive = concave/incised, negative = convex	Terrain profile along the horizontal chord joining the two most distant points of the release-zone boundary; maximum vertical distance between the chord and the profile (+ concave, − convex)	m	Release zone	11.9	11.7	−4.00	45.0
Release-zone curvature	Local surface curvature; positive = convex, negative = concave	Zonal mean of total (standard) DEM curvature (ArcGIS Pro Curvature tool)	ArcGIS curvature units	Release zone	−5.32	16.0	−66.6	33.3
TPI mean	Zonal mean of the Topographic Position Index (local topographic position)	Zonal mean of the Topographic Position Index (ArcGIS Pro; neighbourhood of 10 cells, i.e. 10 m, on the DTM resampled to 1 m)	m	Release zone	0.003	0.007	−0.006	0.033
TPI range	Zonal range (max − min) of the TPI (within-zone topographic heterogeneity)	Zonal max − min of the TPI; neighbourhood as for TPI mean	m	Release zone	5.09	4.28	1.34	20.0
Solar radiation	Mean annual potential incoming solar radiation (Area Solar Radiation)	Zonal mean of potential incoming radiation for the whole year (ArcGIS Pro Area Solar Radiation on the DTM resampled to 1 m; long-term annual mean, default parameters otherwise)	kWh m^{-2} yr^{-1}	Release zone	1009	215	605	1279
Mean path slope	Mean slope gradient of the whole avalanche path	Zonal mean of DEM-derived slope within the whole path polygon	°	Whole path	33.0	4.55	23.6	46.6
Path area	Planimetric area of the avalanche path	Planimetric area of the path polygon (avalanche cadastre)	ha	Whole path	6.58	6.81	0.46	32.7
Vertical drop	Elevation difference between the top of the release zone and the lowest point of the path	DEM elevation difference between the top of the release zone and the lowest point of the path	m	Whole path	295	126	75.0	591
Mean shape index (MSI)	Shape complexity of the path polygon (perimeter relative to an equal-area circle)	$P / (2\sqrt{(\pi A)})$, where P is the perimeter and A the area of the path polygon (1 = circle)	–	Whole path	2.03	0.65	1.08	4.97

Note: All variables were derived in ArcGIS Pro from a 0.5 m digital terrain model (2012) and avalanche-path and release-zone polygons provided by the Krkonoše National Park Administration; TPI mean and range and solar radiation were calculated from the DTM resampled to 1 m. Aspect was transformed into northness and eastness to account for its circular nature. Mean TPI values are close to zero because positive and negative local deviations largely cancel within release zones; within-zone topographic heterogeneity is captured by the TPI range. Variables describing recorded avalanche-event geometry (e.g. event length and width) and redundant terrain measures (maximum release-zone slope, path perimeter, maximum path length and MPAR) were excluded before analysis. The 13 retained variables were z-standardised before PCA.

Table S2. Selection and sensitivity of the avalanche-path morphometric typology. (a) Fusion distances and secondary cluster-validation criteria for four- to six-cluster solutions; (b) agreement between alternative classifications and the final five-cluster typology; (c) Layer B model results using the four-cluster solution, in which C2 and C3 are merged.

Clustering	K	Fusion distance at K→K−1	Increase vs. previous fusion	Cluster sizes	Pseudo-t^2 at K→K−1	Caliński–Harabasz (pseudo-F)	CCC	Silhouette	Davies–Bouldin
Ward-type (ward.D2), Manhattan – final	6	10.80	+0.31	14/9/10/1/5/16	8.24	11.16	−3.13	0.206	1.11
Ward-type (ward.D2), Manhattan – final	5	13.50	+2.70	14/9/11/5/16	7.45	11.57	−1.75	0.218	1.28
Ward-type (ward.D2), Manhattan – final	4	13.72	+0.22	14/20/5/16	12.74	10.76	−1.71	0.192	1.51
Ward, Euclidean – sensitivity	6	6.59	+1.04	7/16/3/12/10/7	7.39	11.49	−2.79	0.233	1.25
Ward, Euclidean – sensitivity	5	7.23	+0.64	7/16/15/10/7	9.01	10.61	−2.68	0.215	1.40
Ward, Euclidean – sensitivity	4	7.53	+0.30	7/16/15/17	13.96	9.66	−2.72	0.190	1.59

Classification variant	Adjusted Rand index vs. final
Ward-type, Manhattan, raw Varimax scores (final C1–C5)	1.00
Ward-type, Manhattan, Kaiser-normalised Varimax scores	0.69
Ward, Euclidean (invariant to rotation)	0.72

Response	Period × Cluster, K = 4	C2 (K = 5)	C3 (K = 5)	C2 + C3 (K = 4)
B1 climatic PC1 (Δ P4−P1)	$\chi^2(9) = 5.75$; $p = 0.765$	+2.02 [−0.27, 4.30]	+2.33 [0.50, 4.16]	+2.02 [0.47, 3.57]
B2 activity (OR P4/P1)	$\chi^2(9) = 33.28$; $p < 0.001$	0.28 [0.05, 1.54]	0.30 [0.07, 1.25]	0.29 [0.08, 1.01]
B3 area (ratio)	$\chi^2(9) = 28.84$; $p < 0.001$	0.78 [0.26, 2.33]	1.18 [0.53, 2.63]	1.04 [0.52, 2.10]
B3 width (ratio)	$\chi^2(9) = 54.70$; $p < 0.001$	0.86 [0.37, 1.97]	0.89 [0.49, 1.62]	0.87 [0.52, 1.46]
B3 length (ratio)	$\chi^2(9) = 15.88$; $p = 0.069$	1.06 [0.60, 1.86]	1.15 [0.76, 1.75]	1.08 [0.74, 1.57]
B3 crown height (ratio)	$\chi^2(9) = 14.44$; $p = 0.107$	0.63 [0.28, 1.39]	1.23 [0.66, 2.30]	0.98 [0.56, 1.70]
B3 deposit height (ratio)	$\chi^2(9) = 8.01$; $p = 0.533$	0.55 [0.27, 1.10]	0.57 [0.33, 0.98]	0.57 [0.35, 0.92]

Note: PCA of 13 z-standardised terrain variables for 55 avalanche paths yielded five components with eigenvalues greater than 1, explaining 70.4 % of total variance (KMO = 0.51; Bartlett's test, $\chi^2(78) = 250.6$, $p < 0.001$). Fusion distance denotes the linkage height at which a K-cluster solution is merged into K − 1 clusters; pseudo-t^2 refers to the same merging step (Duda and Hart, 1973). The Caliński–Harabasz index (pseudo-F; Caliński and Harabasz, 1974), pseudo-t^2 and cubic clustering criterion (CCC; Sarle, 1983) were calculated using within-cluster sums of squares of standardised rotated component scores, while silhouette width was based on the clustering distance. CCC was negative for K = 2–10, and the gap statistic (Tibshirani et al., 2001; 500 reference datasets, Tibshirani SE-max rule) favoured K = 1. These criteria indicate relatively weak separation among groups and were treated as secondary diagnostics. Manhattan distances depend on component rotation, whereas Euclidean distances are invariant under orthogonal rotation. In panel (c), the Layer B models were refitted using the four-cluster solution; estimates for C1, C4 and C5 remained virtually unchanged. Period × Cluster interactions were evaluated using Wald tests for B1 and B2 and likelihood-ratio tests for B3.

Table S3. Sensitivity of the climatic analyses. (a) Layer A: changes in avalanche-day climatic conditions and their effective dimensionality under alternative data specifications; (b) Layer B1: differences in pooled PCA PC1 scores between P1 and P4 by morphometric path type, accounting for repeated climatic observations across cluster-days.

Variant	Period	n	PC1 centroid [95 % CI]	D_eff [95 % CI]	PC1 variance (%)
Main analysis (9 variables; 1999/00–2001/02 excluded)	P1	83	−0.66 [−1.03, −0.26]	5.74 [4.84, 5.99]	31.8
Main analysis (9 variables; 1999/00–2001/02 excluded)	P2	85	−0.31 [−0.67, 0.00]	5.47 [4.54, 5.90]	31.9
Main analysis (9 variables; 1999/00–2001/02 excluded)	P3	94	0.13 [−0.30, 0.86]	4.32 [3.55, 5.49]	41.5
Main analysis (9 variables; 1999/00–2001/02 excluded)	P4	73	0.95 [0.57, 1.32]	4.51 [3.55, 4.88]	38.2
Main analysis (9 variables; 1999/00–2001/02 excluded)	P1 vs. P4	335	Δ = 1.61; p < 0.001	Δ = −1.23; p = 0.025	Δ = +6.5; p = 0.083
Without wind and humidity (6 variables)	P1	83	−0.54 [−0.81, −0.26]	4.84 [4.31, 4.95]	30.6
Without wind and humidity (6 variables)	P2	85	−0.06 [−0.25, 0.07]	4.69 [3.84, 5.01]	32.7
Without wind and humidity (6 variables)	P3	94	0.06 [−0.33, 0.73]	4.00 [3.39, 4.50]	39.1
Without wind and humidity (6 variables)	P4	73	0.62 [0.15, 1.08]	3.95 [3.35, 4.15]	40.6
Without wind and humidity (6 variables)	P1 vs. P4	335	Δ = 1.16; p = 0.001	Δ = −0.89; p = 0.010	Δ = +10.0; p = 0.022
Including 1999/00–2001/02 (382 days)	P1	83	−0.72 [−1.12, −0.31]	5.74 [4.88, 5.99]	31.8
Including 1999/00–2001/02 (382 days)	P2	85	−0.37 [−0.74, −0.06]	5.47 [4.55, 5.88]	31.9
Including 1999/00–2001/02 (382 days)	P3	141	0.17 [−0.20, 0.66]	4.74 [3.99, 5.60]	38.4
Including 1999/00–2001/02 (382 days)	P4	73	0.92 [0.51, 1.28]	4.51 [3.50, 4.89]	38.2
Including 1999/00–2001/02 (382 days)	P1 vs. P4	382	Δ = 1.63; p = 0.001	Δ = −1.23; p = 0.018	Δ = +6.5; p = 0.085

Variant	N	Period × Cluster	C1	C2	C3	C4	C5
Main model (Season random intercept)	436	$\chi^2(12) = 5.53$; p = 0.938	+1.76 [1.00, 2.53]	+2.02 [−0.27, 4.30]	+2.33 [0.50, 4.16]	+0.59 [−1.03, 2.21]	+1.97 [0.90, 3.05]
Weights 1/(path types active on the date)	436	$\chi^2(12) = 8.46$; p = 0.748	+1.77 [1.06, 2.48]	+1.22 [−1.28, 3.71]	+2.30 [0.24, 4.35]	+0.14 [−1.51, 1.78]	+1.87 [0.76, 2.98]
Only dates with one active path type	251	$\chi^2(11) = 10.38$; p = 0.497	+1.91 [1.12, 2.69]	−0.48 [−4.45, 3.49]	+2.44 [−0.80, 5.68]	−0.27 [−2.38, 1.85]	+1.93 [0.38, 3.48]
Main model, whole-winter block-bootstrap CI	436	–	+1.76 [1.08, 2.39]	+2.02 [0.29, 4.36]	+2.33 [1.01, 3.50]	+0.59 [−1.34, 1.61]	+1.97 [0.91, 3.22]

Note: In panel (a), centroids are mean PC1 scores from the pooled PCA fitted separately for each data specification. Confidence intervals were estimated using 2,000 whole-winter block-bootstrap resamples. Effective dimensionality (D_eff) was calculated from the period-specific correlation matrix. P1 versus P4 rows report differences (P4 − P1) and one-sided permutation tests based on 2,000 permutations of complete winters. These tests evaluated directional alternatives: a positive shift in PC1, lower effective dimensionality and a higher PC1 variance share.

In panel (b), 333 unique avalanche dates contributed 436 cluster-days, of which 251 dates involved a single active path type. A Date random intercept could not be estimated because the climatic PC1 score was constant within each date. Weighting by the inverse number of active path types assigned a total weight of one to each date. In the subset of dates with only one active path type, C2 had no observations in P3, so the interaction test had 11 rather than 12 degrees of freedom. Whole-winter bootstrap confidence intervals were based on 999 resamples, of which 905 converged with all Period × Cluster combinations estimable. The main Period × Cluster interaction was $\chi^2(12) = 5.53$, p = 0.938; including the winters 1999/00–2001/02 yielded $\chi^2(12) = 6.71$, p = 0.876, based on 498 cluster-days.

Table S4. Sensitivity of Layer B3 results for avalanche area, width and length to changes in recording precision and restriction to a single valley (Obří důl).

Response	Variant	N	Period × Cluster (LRT)	P4/P1 heterogeneity	C1	C2	C3	C4	C5
Area	R0 main model	790	$\chi^2(12) = 29.20$; $p = 0.004$	$\chi^2(4) = 13.04$; $p = 0.011$	0.38 [0.26, 0.57]	0.78 [0.26, 2.33]	1.18 [0.53, 2.63]	0.50 [0.26, 0.96]	0.62 [0.39, 0.98]
Area	R1 harmonised recording precision	790	$\chi^2(12) = 28.21$; $p = 0.005$	$\chi^2(4) = 11.78$; $p = 0.019$	0.39 [0.26, 0.57]	0.77 [0.26, 2.28]	1.13 [0.51, 2.51]	0.52 [0.27, 1.01]	0.59 [0.37, 0.95]
Area	R4 Obří důl only	299	$\chi^2(6) = 8.80$; $p = 0.185$	$\chi^2(2) = 2.45$; $p = 0.294$	0.47 [0.29, 0.77]	–	0.21 [0.06, 0.69]	0.32 [0.14, 0.74]	–
Width	R0 main model	791	$\chi^2(12) = 58.37$; $p < 0.001$	$\chi^2(4) = 17.67$; $p = 0.001$	0.42 [0.33, 0.54]	0.86 [0.37, 1.97]	0.89 [0.49, 1.62]	0.26 [0.17, 0.42]	0.57 [0.42, 0.78]
Width	R1 harmonised recording precision	791	$\chi^2(12) = 62.07$; $p < 0.001$	$\chi^2(4) = 16.24$; $p = 0.003$	0.42 [0.34, 0.53]	0.86 [0.39, 1.91]	0.85 [0.48, 1.51]	0.28 [0.18, 0.44]	0.56 [0.42, 0.75]
Width	R2 non-rounded widths only	502	$\chi^2(12) = 58.74$; $p < 0.001$	$\chi^2(4) = 15.23$; $p = 0.004$	0.41 [0.32, 0.52]	1.01 [0.37, 2.72]	0.88 [0.48, 1.60]	0.29 [0.17, 0.50]	0.63 [0.45, 0.86]
Width	R4 Obří důl only	299	$\chi^2(6) = 25.10$; $p < 0.001$	$\chi^2(2) = 14.08$; $p < 0.001$	0.47 [0.37, 0.61]	–	0.36 [0.17, 0.74]	0.18 [0.11, 0.29]	–
Length	R0 main model	792	$\chi^2(12) = 19.13$; $p = 0.085$	$\chi^2(4) = 11.27$; $p = 0.024$	0.76 [0.63, 0.91]	1.06 [0.60, 1.86]	1.15 [0.76, 1.75]	1.09 [0.78, 1.52]	0.95 [0.76, 1.20]
Length	R1 harmonised recording precision	792	$\chi^2(12) = 19.13$; $p = 0.086$	$\chi^2(4) = 10.92$; $p = 0.027$	0.75 [0.62, 0.91]	1.06 [0.60, 1.86]	1.14 [0.76, 1.73]	1.07 [0.77, 1.49]	0.94 [0.74, 1.18]
Length	R4 Obří důl only	299	$\chi^2(6) = 0.93$; $p = 0.988$	$\chi^2(2) = 0.33$; $p = 0.849$	0.79 [0.61, 1.03]	–	0.91 [0.48, 1.73]	0.86 [0.56, 1.34]	–

Note: P4/P1 ratios and 95 % confidence intervals were estimated using linear mixed-effects models of log-transformed avalanche-event measurements, with crossed Path, Season and Date random intercepts fitted by restricted maximum likelihood. Period × Cluster interactions were evaluated using likelihood-ratio tests based on maximum-likelihood fits, and differences among path types in P4/P1 ratios using Wald tests.

R0 denotes the main model. In R1, width and length were harmonised to the recording precision used before 2009/10 (10 m and 50 m, respectively), and avalanche area was adjusted by the ratio of harmonised to original width–length products. R2 includes only events with widths not divisible by 50 m, because widths in early records were frequently rounded to 50 m. R4 is restricted to Obří důl, where only C1, C3 and C4 occur. Adding a locality (cirque or valley) random intercept (R3) produced a zero variance estimate and did not change the results; this variant is therefore not shown.

Table S5. Avalanche paths with no recorded natural avalanche in P1 and sensitivity of the Layer B2 path-activity results to their exclusion.

Path	Name	Cluster	Natural avalanches	First recorded winter	Avalanches P2 / P3 / P4
1	Žlaby Sněžky	C3	6	2001/02	0 / 4 / 2
11A	Pramenný důl	C2	5	2004/05	0 / 3 / 2
11B	Pramenný důl	C3	2	2005/06	0 / 2 / 0
16	Borůvkový žlab	C5	5	1993/94	2 / 2 / 1
16A	Stoh1	C5	1	2011/12	0 / 0 / 1
16B	Stoh2	C5	1	2011/12	0 / 0 / 1
40	Richterovi boudy	C2	1	2011/12	0 / 0 / 1
6C	Murová dráha	C4	4	2001/02	0 / 2 / 2

Variant	N	Period × Cluster	C1	C2	C3	C4	C5
All 55 paths	2310	$\chi^2(12) = 33.92$; $p < 0.001$	0.11 [0.04, 0.32]	0.28 [0.05, 1.54]	0.30 [0.07, 1.25]	0.57 [0.15, 2.21]	0.41 [0.14, 1.25]
Without paths inactive in P1 (n = 8)	1974	$\chi^2(12) = 37.00$; $p < 0.001$	0.11 [0.03, 0.32]	–	0.19 [0.04, 0.90]	0.39 [0.10, 1.63]	0.33 [0.11, 1.03]
Without Murová dráha (6C)	2268	$\chi^2(12) = 32.69$; $p = 0.001$	0.11 [0.04, 0.32]	0.29 [0.05, 1.60]	0.31 [0.07, 1.29]	0.39 [0.10, 1.60]	0.42 [0.14, 1.26]

Note: Eight avalanche paths had no recorded natural avalanche during P1 (1978/79–1988/89). The Layer B2 model was refitted for all 55 paths, after excluding these eight paths and after excluding Murová dráha (path 6C) alone. Estimates are P4/P1 odds ratios with 95 % confidence intervals. A dash indicates a non-estimable contrast. After exclusion of the eight paths, B1 and B3 could not be estimated because several Period × Cluster combinations contained no observations. Excluding Murová dráha alone produced only small changes in B1 and B3 estimates (largest difference: C4 avalanche-area ratio, 0.50 to 0.55). The first recorded avalanche on a path does not necessarily indicate its physical formation.

Table S6. Frequency and share of large natural avalanche events across the four study periods.

Definition	P1	P2	P3	P4	Frequency: LRT Period	Rate ratio P4/P1	Share: LRT Period
Area > 5.0 ha (75th percentile)	7.1 (36 %)	3.0 (23 %)	7.1 (21 %)	1.5 (15 %)	$\chi^2(3) = 9.94$; $p = 0.019$	0.21 [0.07, 0.59]	$\chi^2(3) = 9.53$; $p = 0.023$
Area > 8.1 ha (90th percentile)	1.8 (9 %)	1.4 (11 %)	3.7 (11 %)	0.6 (6 %)	$\chi^2(3) = 6.12$; $p = 0.106$	0.35 [0.09, 1.40]	$\chi^2(3) = 0.45$; $p = 0.930$
Area ≥ 0.5× path area	9.5 (49 %)	4.7 (36 %)	14.2 (42 %)	3.0 (31 %)	$\chi^2(3) = 12.53$; $p = 0.006$	0.31 [0.13, 0.74]	$\chi^2(3) = 7.06$; $p = 0.070$
Area ≥ 1× path area (overrun)	2.2 (11 %)	2.1 (16 %)	6.2 (18 %)	1.4 (14 %)	$\chi^2(3) = 5.67$; $p = 0.129$	0.63 [0.17, 2.36]	$\chi^2(3) = 1.08$; $p = 0.782$

Note: For P1–P4, values show the mean number of large avalanche events per winter, with their percentage share among all recorded natural avalanches in parentheses. Absolute area thresholds are based on the 800 of 807 natural avalanches with recorded area; path-relative thresholds use the 790 events with recorded area assigned to mapped avalanche paths. Frequency was analysed using negative-binomial generalised linear models of winter event counts (42 winters), with overall Period effects evaluated by likelihood-ratio tests. Rate ratios compare P4 with P1. Event shares were analysed using binomial mixed-effects models with Path and Season random intercepts. Overall Period tests and P4/P1 rate ratios represent different statistical comparisons.

Table S7. Changes in tree cover between 1953 and 2024 within avalanche paths and in their surroundings, for all paths and by morphometric path type (area-weighted).

Zone	Cluster	Zone area (ha)	Tree area 1953 (ha)	Tree area 2024 (ha)	Tree cover 1953 (%)	Tree cover 2024 (%)	Change (pp)
Avalanche path	All	368.3	45.5	62.4	12.4	17.0	+4.6
Avalanche path	C1	230.3	35.4	42.0	15.4	18.2	+2.9
Avalanche path	C2	32.0	0.5	2.7	1.7	8.3	+6.6
Avalanche path	C3	49.2	2.9	8.0	5.8	16.3	+10.5
Avalanche path	C4	12.5	3.6	3.3	29.0	26.2	−2.8
Avalanche path	C5	44.3	3.1	6.5	7.1	14.7	+7.6
0–25 m around the path	All	202.2	65.2	89.2	32.2	44.1	+11.9
0–25 m around the path	C1	81.1	28.6	35.6	35.2	43.9	+8.7
0–25 m around the path	C2	20.8	2.8	5.8	13.3	27.8	+14.5
0–25 m around the path	C3	44.2	12.3	21.5	27.8	48.7	+20.9
0–25 m around the path	C4	16.1	8.1	9.6	50.4	59.8	+9.4
0–25 m around the path	C5	39.9	13.5	16.6	33.7	41.7	+8.0
25–50 m around the path	All	211.6	81.1	104.8	38.3	49.5	+11.2
25–50 m around the path	C1	82.5	33.6	41.3	40.7	50.1	+9.4

Zone	Cluster	Zone area (ha)	Tree area 1953 (ha)	Tree area 2024 (ha)	Tree cover 1953 (%)	Tree cover 2024 (%)	Change (pp)
25–50 m around the path	C2	24.0	4.3	7.3	17.7	30.6	+12.8
25–50 m around the path	C3	46.3	18.9	26.2	40.8	56.6	+15.8
25–50 m around the path	C4	17.3	9.5	11.6	54.9	67.0	+12.1
25–50 m around the path	C5	41.5	14.8	18.4	35.7	44.2	+8.5

Note: Tree cover is expressed as the percentage of the corresponding spatial zone occupied by mapped mature trees (union of manually vectorised tree polygons of 3 m² or larger; 1953 orthophoto and 2024 ČÚZK orthophoto). Changes are reported in percentage points (pp), not as relative percentage changes. The surrounding zones extend 0–25 m and 25–50 m beyond the mapped avalanche paths. Values are area-weighted across paths within each type. Dwarf pine and young trees were excluded from the mapping.

Year × Cluster interaction (linear mixed-effects model with a Path random intercept, likelihood-ratio test): avalanche path $\chi^2(4) = 9.32$, $p = 0.054$; 0–25 m $\chi^2(4) = 14.11$, $p = 0.007$; 25–50 m $\chi^2(4) = 7.45$, $p = 0.114$. Paired Wilcoxon tests of per-path change: path vs. 0–25 m $V = 194$, $p < 0.001$; path vs. 25–50 m $V = 347$, $p = 0.005$.

Supplementary references

Caliński, T. and Harabasz, J.: A dendrite method for cluster analysis, Communications in Statistics, 3, 1–27, https://doi.org/10.1080/03610927408827101, 1974.

Duda, R. O. and Hart, P. E.: Pattern classification and scene analysis, Wiley, New York, 1973.

Sarle, W. S.: Cubic clustering criterion, SAS Technical Report A-108, SAS Institute, Cary, NC, 1983.

Tibshirani, R., Walther, G., and Hastie, T.: Estimating the number of clusters in a data set via the gap statistic, Journal of the Royal Statistical Society: Series B (Statistical Methodology), 63, 411–423, https://doi.org/10.1111/1467-9868.00293, 2001.